

# JetViP 1.1: Calculating One- and Two-Jet Cross Sections with Virtual Photons in NLO QCD

B. Pötter

II. Institut für Theoretische Physik\*, Universität Hamburg  
Luruper Chaussee 149, D-22761 Hamburg, Germany  
e-mail: poetter@mail.desy.de

## Abstract

**JetViP** is a computer program for the calculation of inclusive single- and di-jet cross sections in  $eP$ - and  $e\gamma$ -scattering in NLO QCD. The virtuality of the photon, radiated by the incoming electron, can be chosen in a continuous range, reaching from photoproduction into deep inelastic scattering. The various contributions to the full jet cross section, including the resolved photon contributions, are implemented. The calculation is based on the phase-space-slicing method.

---

\*Supported by Bundesministerium für Forschung und Technologie, Bonn, Germany, under Contract 05 7 HH 92P (0), and by EEC Program *Human Capital and Mobility* through Network *Physics at High Energy Colliders* under Contract CHRX-CT93-0357 (DG12 COMA).

## PROGRAM SUMMARY

*Titel of the program:* **JetViP** version 1.1.

*Computer-Environment:* Any machine running standard **FORTRAN 77**. **JetViP** has been especially tested on HP-Clusters, IRIX-machines and Linux PCs.

*Programming language used:* **FORTRAN 77**.

*High speed storage required:* Size of executable program is approximately 9 MBytes.

*Other programs used:* **VEGAS** (multidimensional Monte Carlo integration routine), **PDFLIB**, **SaSgam**, **GRS** (parametrizations of parton densities).

*Keywords:* Quantum Chromodynamics (QCD), Jet Physics, Deeply Inelastic Electron-Proton ( $eP$ ) and Electron-Photon ( $e\gamma$ ) Scattering (DIS), Photoproduction, Transition from Photoproduction to DIS.

*Nature of physical problem:* In  $eP$ - and  $e\gamma$ -scattering experiments, the hadronic final state can be analysed by jet cluster algorithms, yielding inclusive single- and dijet cross sections. These can be obtained in a continuous range of photon virtuality. The cross sections allow the extraction of parameters, such as  $\alpha_s$ ,  $\Lambda_{\overline{\text{MS}}}$  or parton densities (also of the virtual photon), if the respective jet cross sections are theoretically known.

*Method of solution:* **JetViP** is a computer program for the calculation of inclusive single- and dijet cross sections in  $eP$ - and  $e\gamma$ -scattering in NLO QCD. The virtuality of the photon, radiated by the incoming electron, can be chosen in a continuous range, reaching from photoproduction into deep inelastic scattering. The various contributions to the full jet cross section, including the resolved photon contributions, are implemented. The calculation is based on the phase-space-slicing method.

*Typical running time:* Varies strongly from LO to NLO and depends on type of subprocess (direct or resolved). At LO, running times of about 1 minute for a cross section with fixed bin-size in one of the kinematical variables are typical. At NLO, the running time for such a cross section varies between 30 minutes (for the single resolved contributions) to 5 hours (for the double resolved contributions).

# 1 Introduction

One possibility to analyze hadronic final states in high energy collision experiments is to cluster the final state particles into jets with large transverse energy  $E_T$ , using a specific cluster algorithm. In this way, inclusive single- and dijet cross sections can be obtained for various physical processes. At HERA, jet cross sections in electron-proton scattering have been experimentally accessible for two distinct regions of the virtuality  $Q^2$  of the photon radiated by the lepton; one region is that of nearly on-shell photons ( $Q^2 \simeq 0$ ) [1, 2, 3], the other is that of photons with very large virtuality,  $Q^2 \gg 10 \text{ GeV}^2$  [4, 5]. These two regions define the photoproduction and the deep inelastic scattering (DIS) regimes, respectively. On the theoretical side, perturbative QCD calculations are possible due to the presence of a large scale in these processes and single- and dijet cross sections have been calculated in next-to-leading order (NLO) for both regimes. Two different methods for these higher order perturbative calculations have been used. In the phase space slicing method, the singular phase space regions of soft and collinear final state particles are separated by introducing an invariant mass cut-off  $y_s$ . The finite phase space regions outside the cut-off are calculated numerically. This method has been used in photoproduction [6, 7, 8] and in DIS [9, 10]. The subtraction method on the other hand is based on a point-by-point subtraction of singularities in the numerical integration. This method has also been applied in photoproduction [11] and DIS [12, 13].

Recently, the gap in  $Q^2$  between photoproduction and DIS is being closed by experiment and data becomes available for  $eP$ -scattering in the region of intermediate photon virtuality, i.e., for  $Q^2 \simeq [0, 100] \text{ GeV}^2$  [14, 15]. This has triggered theoretical studies that try to match the photoproduction and DIS regimes and to provide a unified approach to treat virtual photons in a continuous  $Q^2$ -range. From photoproduction it is well-known that the real photon does not only interact directly with the partons from the proton, but that it can also serve as a source of partons, i.e., quarks and gluons. These contributions are called *direct* and *resolved*, respectively. The resolved component is accompanied by a small  $E_T$  remnant jet. In DIS, the resolved contribution should vanish. Thus, one problem in matching the low and the high  $Q^2$  regions is to construct a parton distribution function (PDF) of the virtual photon, which has been done by Glück, Reya and Stratmann (GRS) [16] and Schuler and Sjöstrand (SaS) [17]. However, only limited data exist for the virtual photon structure function; older measurements have been performed by the PLUTO collaboration at the  $e^+e^-$  collider facility PETRA [18]. Therefore, the available virtual photon PDF's inhibit a rather larger uncertainty in shape and magnitude, especially in the region of small  $x$ . Drees and Godbole [19] have invented a simple  $Q^2$ -dependent interpolation factor which multiplies the PDF's of the real photon.

Another theoretical question is how jet cross sections can be calculated for all  $Q^2$ , which has been addressed in a number of works using leading order (LO) matrix elements [20, 21]. However, LO calculations suffer from large scale and scheme dependences and are insensitive to any kind of jet clustering algorithm. These problems can only be cured in NLO QCD. In NLO photoproduction one has to subtract the initial state singularities arising

from the photon to quark-antiquark splitting and absorb them into the photon structure function, which introduces a factorization scale dependence in the direct and resolved components. The collinear parton from the photon splitting will produce a low  $E_T$  jet, similar to the remnant jet of the resolved component. Therefore, the separation of the direct and resolved processes is no longer possible in NLO. The results from photoproduction can be extended to photons with moderate virtuality. The subtraction of photon initial state singularities for virtual photons has been worked out using the phase space slicing method in [22, 23]. The subtraction term is absorbed into the  $Q^2$ -dependent virtual photon structure function. The NLO calculations for virtual photons with direct and resolved components have been completed in [24] by including the longitudinally polarized direct photon contribution.

In the near future, measurements of jet cross sections from  $e\gamma$ -scattering in a  $Q^2$ -range of the virtual photon similar to that at HERA will become available at LEP2 [25, 26] which complements the HERA measurements. From the theoretical side, the problems to be addressed in  $e\gamma$ -scattering are very similar to those in  $eP$ -scattering, since the same types of subprocesses are encountered. An extra contribution from the direct interaction of the real and the virtual photon has to be considered. These contributions have been worked out in [23, 27].

The goal of this paper is to describe how the calculations in [22, 23, 24, 27] are implemented in the computer package **JetViP**<sup>1</sup> for calculating jet cross sections in NLO QCD with virtual photons. This program provides a link between the DIS and the photoproduction regimes. The NLO calculations in deep-inelastic  $eP$ -scattering have been implemented in several other computer programs. The program **MEPJET** [9] uses the phase space slicing method, whereas **DISENT** [12] and **DISASTER++** [28] use the subtraction method. Two different strategies have been applied in the programs for calculating jet cross sections. In **MEPJET**, a complete package is provided to handle the convolution of the hard, perturbatively calculable partonic cross sections with the parton density functions in the initial state and the recombination of final state partons from the subprocess to jets. For obtaining final jet cross sections, only a steering file has to be manipulated. In contrast, **DISENT** and **DISASTER++** generate an event of final state partons, weighted with the respective hard scattering cross section. The convolution over the initial state and the recombination of the partons in the final state into jets is left to the user. Of course, this allows a high flexibility, since any jet recombination or kinematical cut can be implemented. The disadvantage is that the user will have to do a lot of programming before jet cross sections can be calculated. A number of NLO programs exist also for the case of photoproduction in  $eP$ - and  $\gamma\gamma$ -scattering [6, 7, 8, 11], but these have not been published yet. It should be mentioned that cross checks of **JetViP** with existing programs in DIS and photoproduction have been performed which showed good agreement [30].

For the sake of being user-friendly, in **JetViP** we have adopted the strategy used in **MEPJET**. All stages of the calculation are implemented in the program. In particular we

---

<sup>1</sup>**JetViP** is an acronym for: **J**ets with **V**irtual **P**hotons.

use the cone algorithm according to the Snowmass standard [29] for combining partons in the final state into jets with radius  $R$ . We use however the  $R_{sep}$  parameter to modify the Snowmass algorithm to allow a higher flexibility for comparison with experiments. Especially it is possible to simulate  $k_{\perp}$ -like algorithms, containing an  $R$  parameter. One feature of **JetViP** is that the transverse energies and rapidities of the jets are accessible so that cuts on these variables can be applied. By choosing a zero cone radius, i.e.,  $R = 0$ , the transverse energies and rapidities of the partons, rather than those of the jets, are accessible and thus other jet recombination schemes than the two mentioned here can be implemented by the user. Finally,  $\gamma^*\gamma$ -scattering from  $e^+e^-$  colliders can be studied with **JetViP**. I will restrict myself in this paper to explaining the computational techniques implemented in the package and the general structure of the program. Physical applications have been discussed elsewhere [22, 23, 24, 27, 30]. There, also the details of the NLO calculations can be found.

The outline of the paper is as follows. In section 2 the process of  $eP$ -scattering is discussed and the phase space slicing method is explained. Details of the subtraction of the virtual photon initial state contribution, which is vital for connecting the DIS and the photoproduction limits, are given and the iterative cone algorithm is discussed. In section 3 these results are extended to photon-photon scattering. The input parameters of the steering file are defined in section 4 and the range of the input parameters is discussed. Last, section 5 contains a guide for the installation of **JetViP** on different computer platforms. Furthermore, typical running times are given. The appendices contain examples of the input- and output-files, which can be used as simple cross checks after installation of the program.

## 2 Jet Cross Sections in Electron-Proton Scattering

### 2.1 General Structure of Cross Sections

In order to define the general structure of the cross sections which can be calculated with **JetViP**, we write for the inclusive production of two jets in electron-proton scattering

$$e(k) + P(p) \rightarrow e(k') + \text{jet}_1(E_{T_1}, \eta_1) + \text{jet}_2(E_{T_2}, \eta_2) + X \quad . \quad (1)$$

Here,  $k$  and  $p$  are the momenta of the incoming electron and proton, respectively and  $k'$  is the momentum of the outgoing electron. The two jets in the final state are characterized by their transverse momenta  $E_{T_i}$  and rapidities  $\eta_i$ , which are the observables also in the experiment. The four-momentum transfer of the electron is  $q = k - k'$  and  $Q^2 = -q^2$ . The phase space of the electron is parametrized by the invariants  $y = pq/pk$  and  $Q^2$ . In **JetViP** a continuous range in  $Q^2$  is covered. In the case of very small virtualities  $Q^2 \ll q_0^2$ , where  $q_0$  is the energy of the virtual photon,  $y$  gives the momentum fraction of the initial electron energy  $k_0$ , carried away by the virtual photon and  $y = q_0/k_0$ . The total energy

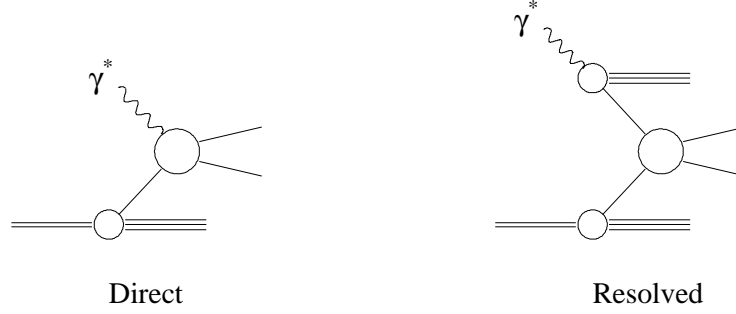


**Figure 1:** The direct and resolved contributions in  $\gamma^*P$ -scattering.

in the  $eP$  center-of-mass system (c.m.s.) is  $\sqrt{S_H}$ , where  $S_H = (k + p)^2$ .  $W$  denotes the energy in the virtual photon-proton ( $\gamma^*P$ ) subsystem,  $W^2 = (q + p)^2$ .

As already mentioned in the introduction, in photoproduction, i.e., for  $Q^2 \simeq 0$ , the photon can not only interact directly with the partons from the proton, but can also have a non-perturbative, resolved structure which has to be described by a structure function. The concept of resolved photons can be extended to virtual photons with moderate virtuality. In **JetViP**, the direct and resolved components for the virtual photon, shown in Fig. 1, are implemented. In the following I will describe how cross sections for the direct and resolved components in deep inelastic  $eP$ -scattering are calculated with **JetViP**, starting with the familiar direct case.

The hadronic cross section  $d\sigma^H$  for the direct interaction is written as a convolution of the hard scattering cross section  $d\sigma_{eb}$ , where the electron interacts with the parton  $b$  originating from the proton, parametrized by the PDF of the proton  $f_{b/P}(x_b)$  with  $x_b$  denoting the parton momentum fraction, so that

$$d\sigma^H(S_H) = \sum_b \int dx_b d\sigma_{eb}(x_b S_H) f_{b/P}(x_b) \quad . \quad (2)$$

The cross section  $d\sigma_{eb}$  for the scattering of the electron on the parton  $b$  is related to the lepton and hadron tensors  $L_{\mu\nu}$  and  $H_{\mu\nu}$  by

$$d\sigma_{eb} = \frac{1}{4S_H x_b} \frac{4\pi\alpha}{Q^4} L^{\mu\nu} H_{\mu\nu} d\text{PS}^{(n)} dL \quad . \quad (3)$$

Here,

$$dL = \frac{Q^2}{16\pi^2} \frac{d\phi dy dQ^2}{2\pi Q^2} \quad (4)$$

depends only on the electron variables, whereas  $d\text{PS}^{(n)}$  depends only on the  $n$  final state particles from the hard interaction. The azimuthal angle of the outgoing electron in the hadronic c.m.s.,  $\phi$ , is integrated out in  $d\sigma_{eb}$  with the result

$$d\overline{\sigma}_{eb} = \int_0^{2\pi} d\phi \frac{d\sigma_{eb}}{d\phi} = \frac{\alpha}{2\pi} \left( \frac{1 + (1-y)^2}{y} d\sigma_{\gamma b}^U + \frac{2(1-y)}{y} d\sigma_{\gamma b}^L \right) \frac{dy dQ^2}{Q^2} \quad . \quad (5)$$

In this formula the cross sections for the scattering of transversely unpolarized and longitudinally polarized virtual photons on the parton  $b$  are given by

$$d\sigma_{\gamma b}^U = \frac{1}{4x_b S_H y} (H_g + H_L) d\text{PS}^{(n)} \quad , \quad (6)$$

$$d\sigma_{\gamma b}^L = \frac{1}{2x_b S_H y} H_L d\text{PS}^{(n)} \quad , \quad (7)$$

with the definitions  $H_g = -g^{\mu\nu} H_{\mu\nu}$  and  $H_L = \frac{4Q^2}{(S_H y)^2} p^\mu p^\nu H_{\mu\nu}$ . In the limit  $Q^2 \rightarrow 0$  one obtains the familiar formula for the absorption of photons with small virtuality, where  $d\sigma_{\gamma b}^L$  is neglected and the transversely unpolarized cross section  $d\sigma_{\gamma b}^U$  is multiplied with the differential Weizsäcker-Williams spectrum

$$\frac{df_{\gamma/e}}{dQ^2} = \frac{\alpha}{2\pi} \frac{1 + (1 - y)^2}{y Q^2} \quad . \quad (8)$$

When a photoproduction cross section is calculated with **JetViP**, where  $Q^2 \simeq 0$ , formula (8) is integrated over a small  $Q^2$ -range, from  $Q_{min}^2 = m_e^2 y^2 / (1 - y)$  up to a certain fixed  $Q_{max}^2$ . For all other  $Q^2 > 0$ , the full formula (5) is used instead of this approximation, in particular the longitudinal cross section is included, which can account for up to 50% of the full cross section, depending on the kinematical conditions. The formula (5) does not involve any approximations, except that terms proportional to  $m_e^2$  are neglected.

We now turn to the case, where a photon with moderate virtuality interacts with the parton  $b$  from the proton not as a point-like particle, but via the partonic constituents of the photon. This partonic structure of the photon is described by PDF's  $f_{a/\gamma}^{U,L}(x_a)$ , introducing the new variable  $x_a$  which gives the momentum fraction of the parton in term of the virtual photon momentum,  $p_a = x_a q$ . Since we must distinguish between transversely and longitudinally polarized photons in (5), we must introduce two PDF's for the photon with label U and L. To simplify the formalism we can include the case of the direct photon interaction in the PDF's of the photon by using  $f_{\gamma/\gamma}^{U,L} = \delta(1 - x_a)$  in the formula below. Taking everything together, the hadronic cross section  $d\bar{\sigma}_H(S_H)$  can be written as a convolution of the hard scattering cross section  $d\sigma_{ab}$  for the reaction  $a + b \rightarrow \text{jet}_1 + \text{jet}_2 + X$  with the PDF's of the photon  $f_{a/\gamma}^{U,L}(x_a)$  and the proton  $f_{b/P}(x_b)$  in the following form

$$\frac{d\bar{\sigma}_H(S_H)}{dQ^2 dy} = \sum_{a,b} \int dx_a dx_b f_{b/P}(x_b) d\bar{\sigma}_{ab} \frac{\alpha}{2\pi Q^2} \left[ \frac{1 + (1 - y)^2}{y} f_{a/\gamma}^U(x_a) + \frac{2(1 - y)}{y} f_{a/\gamma}^L(x_a) \right] \quad . \quad (9)$$

Of course, for the direct photon interaction  $f_{a/\gamma}^{U,L} d\sigma_{ab} = \delta(1 - x_a) d\sigma_{\gamma b}^{U,L}$ . At this point we mention that only the unpolarized PDF  $f_{a/\gamma}^U$  is implemented in **JetViP**, for reasons that will become clear in section 2.3. For the longitudinal PDF  $f_{a/\gamma}^L$  only the delta function part is taken into account.

Since cross sections in **JetViP** are calculated in the hadronic c.m.s., i.e., where the incoming photon and hadron are collinear, at least two jets have to be present in the final

Table 1: Two-body subprocesses (Born and virtual) implemented in **JetViP**.

direct	resolved		
$\gamma^* q \rightarrow qq$	$qq' \rightarrow qq'$	$qq \rightarrow qq$	$qg \rightarrow qq$
$\gamma^* g \rightarrow q\bar{q}$	$q\bar{q}' \rightarrow q\bar{q}'$	$q\bar{q} \rightarrow q\bar{q}$	$gg \rightarrow gg$
	$q\bar{q} \rightarrow q'\bar{q}'$	$q\bar{q} \rightarrow gg$	$gg \rightarrow q\bar{q}$

Table 2: Three-body NLO subprocesses implemented in **JetViP**.

direct	resolved		
$\gamma^* q \rightarrow qgg$	$qq' \rightarrow qq'g$	$qq \rightarrow qqg$	$q\bar{q} \rightarrow ggg$
$\gamma^* g \rightarrow q\bar{q}g$	$q\bar{q}' \rightarrow q\bar{q}'g$	$q\bar{q} \rightarrow q\bar{q}g$	$gg \rightarrow q\bar{q}g$
$\gamma^* q \rightarrow qq\bar{q}$	$q\bar{q} \rightarrow q'\bar{q}'g$	$qg \rightarrow qq\bar{q}$	$gg \rightarrow ggg$
$\gamma^* q \rightarrow qq'\bar{q}'$	$qg \rightarrow qq'\bar{q}'$	$qg \rightarrow qqg$	

state due to momentum conservation. Thus, the LO cross section on the parton level has two partons in the final state. The NLO corrections consist of the one-loop contributions with two partons in the final state and the real corrections with three partons in the final state. The different kind of subprocesses implemented in **JetViP** for the direct and resolved cross sections are listed for the two-body final states in Tab. 1. These contain the LO Born contributions, if no internal loops are present, and the NLO virtual corrections. The three-body contributions are listed in Tab. 2 and are NLO. The direct contributions contain both the transverse and the longitudinal photon polarizations. The direct contributions implemented in **JetViP** are taken from Graudenz [10], the resolved contributions are taken from Klasen, Kleinwort and Kramer [6]. The  $Z^0$ -exchange, which is negligible for  $Q^2 \ll M_Z^2$ , is not implemented in **JetViP**. In the following section we explain how the NLO partonic cross sections are calculated in principle with the phase space slicing method.

## 2.2 Partonic Cross Sections in NLO QCD

The LO cross section  $d\sigma^B$  on the parton level consists of the Born matrix elements and a two-parton phase space. The NLO QCD corrections to the LO cross section consist of the



virtual corrections  $d\sigma^V$  with a two-parton final state and the real corrections, where an additional parton is radiated. Both these contributions have characteristic divergencies.

The virtual corrections have infrared and ultraviolet singularities due to the integration over the internal loops, which have been calculated with the help of dimensional regularization. The ultraviolet singularities are regularized in  $d = 4 - 2\epsilon$  space-time dimensions and subtracted in the modified minimal subtraction ( $\overline{\text{MS}}$ ) scheme. The infrared divergences produce  $\epsilon^{-n}$ -terms, which become singular in the limit  $\epsilon \rightarrow 0$ . These cancel against poles in the real corrections.

The real corrections  $d\sigma^R$  are singular in regions where one of the outgoing partons is soft or collinear. These singular phase-space regions are separated from the finite regions by applying the phase-space slicing method [6]. To illustrate the method, we write down the integration of over the phase-space of the third particle, somewhat symbolically, as

$$d\sigma^R = \int_0^1 d\text{PS}^{(3)} |\mathcal{M}_{2 \rightarrow 3}|^2 = \int_0^{y_s} d\text{PS}^{(3)} |\mathcal{M}_{2 \rightarrow 3}|^2 + \int_{y_s}^1 d\text{PS}^{(3)} |\mathcal{M}_{2 \rightarrow 3}|^2 \quad (10)$$

where we have inserted a technical slicing parameter  $y_s$  to separate different regions of phase space. The first integral on the rhs of this equation, which we denote as  $d\sigma_2(y_s)$ , contains the singular parts, where one of the final state particles becomes soft or collinear and can not be observed. To integrate the singular piece  $d\sigma_2$ , the three-body phase space is split into a two-body phase space (of the two remaining particles) and a singular phase space  $d\text{PS}^{(s)}$ , which is integrated out using dimensional regularization, as for the virtual corrections. Effectively a two-parton final state remains:

$$d\sigma_2(y_s) = d\text{PS}^{(2)} \int_0^{y_s} d\text{PS}^{(s)} |\mathcal{M}_{2 \rightarrow 3}|^2 \quad . \quad (11)$$

The second integral, which we denote as  $d\sigma_3(y_s)$ , is finite due to the cut-off at the lower integration boundary. **JetViP** integrates out  $d\sigma_3$  numerically using the Monte-Carlo integration package **VEGAS** [31] to handle the multi-dimensional phase-space integrals. In the numerical part, a variety of experimental cuts and jet definitions can be implemented. This flexibility allows a detailed comparison between theory and experiment. The  $y_s$ -dependence of  $d\sigma_3(y_s)$  has to cancel against that of the two-body contributions  $d\sigma_2(y_s)$ , so that the NLO real corrections,  $d\sigma^R = d\sigma_2(y_s) + d\sigma_3(y_s)$ , are independent of  $y_s$ . In the actual calculation of  $d\sigma_2$ , contributions of order  $\mathcal{O}(y_s \ln^n y_s)$  are neglected, so  $y_s$  has to be chosen sufficiently small in the numerical part  $d\sigma_3$  for the cancellation to be valid.

The two-body part of the real corrections can be further distinguished into initial state and final state corrections,  $d\sigma_2 = d\sigma^I + d\sigma^F$ , where a particle in the initial or final state produces a singularity. The infrared poles in  $d\sigma_2$  are canceled by poles from the virtual corrections, except for simple poles in  $\epsilon$  from the initial state which are multiplied by a splitting function  $P_{a \leftarrow b}$ . The singular terms are absorbed into the scale dependent

structure function of the hadron  $H$  the initial parton was emitted from:

$$f_{a/H}(\eta, M_F^2) = \int_{\eta}^1 \frac{dz}{z} \left( \delta_{ab} \delta(1-z) + \frac{\alpha_s}{2\pi} \Gamma_{a \leftarrow b}^{(1)}(z, M_F^2) \right) f_{b/H} \left( \frac{\eta}{z} \right) , \quad (12)$$

where  $f_{b/H}$  is the LO PDF before the absorption of the collinear singularity and  $M_F^2$  is the factorization scale. The transition function  $\Gamma_{a \leftarrow b}^{(1)}(z)$  contains the pole term and some finite part  $C_{a/b}$ , which is chosen to be zero in the  $\overline{\text{MS}}$  scheme:

$$\Gamma_{a \leftarrow b}^{(1)}(M_F^2)(z) = -\frac{1}{\epsilon} P_{a \leftarrow b}(z) \left( \frac{4\pi\mu^2}{M_F^2} \right)^{\epsilon} \frac{\Gamma(1-\epsilon)}{\Gamma(1-2\epsilon)} + C_{a/b}(z) . \quad (13)$$

The  $\epsilon$ -dependent factors are artefacts of the dimensional regularization. The renormalized initial state cross section  $d\sigma^I$  is calculated from the unrenormalized cross section  $d\bar{\sigma}^I$  by subtracting the singular terms convoluted with the Born cross section:

$$d\sigma_{ab}^I = d\bar{\sigma}_{ab} - \frac{\alpha_s}{2\pi} \int dz \Gamma_{b \leftarrow b'}^{(1)}(z, M_F^2) d\sigma_{ab'}^B . \quad (14)$$

After this subtraction procedure, the sum of all LO and NLO two-body contributions

$$d\sigma^B + d\sigma^V + d\sigma_2(y_s) = d\sigma^B + d\sigma^V + d\sigma^I(y_s) + d\sigma^F(y_s) \quad (15)$$

is finite and the limit  $\epsilon \rightarrow 0$  can be safely performed. Adding the two-body contributions and the three-body contributions  $d\sigma_3(y_s)$  then yields a physically meaningful NLO cross section, which is finite and independent of  $y_s$ .

Since the subtraction of initial state contributions for the virtual photon is of special interest for the transition from photoproduction to DIS, I will explain this point in more detail in the following section.

## 2.3 Subtraction of Virtual Photon Initial State Contributions

In JetViP two different concepts for calculating jet cross sections in  $eP$ -scattering for finite  $Q^2$  are realized:

1. The virtual photon couples directly to the partons from the proton, which reflects the classical situation known as deep-inelastic scattering. The integration of the NLO matrix elements over the three-body final state is not truncated on the virtual photon side at a small cut-off  $y_s$ , since all contributions are finite. They may, however, be large for  $Q^2 \ll E_T^2$ .
2. Large logarithms from the virtual photon side (for  $Q^2 \ll E_T^2$ ) are separated from contributions where the photon couples directly to the partons from the proton by introducing a lower integration boundary  $y_s$  in the phase space integrations of the three-body final state. These logarithms are absorbed into the virtual photon structure function. Therefore one has to add a resolved contribution, where the photon serves as a source of partons that interact with the partons from the proton.

Since it is a priori not clear up to which virtualities the concept of a resolved virtual photon makes sense, always both approaches should be considered for comparison. Normally, this would require two separate calculations, one for each approach, since the phase space integrations are truncated in the numerical part for the second approach. However, as will become clear in the following, the subtraction term can be calculated separately, so that no additional CPU time is required.

We start by reminding that the real, i.e., massless, photon can decay into a quark-antiquark pair in the initial state, which becomes collinear and produces a singularity. The subtraction of photon initial state singularities for the real photon has been worked out in the phase space slicing method in [6]. The procedure for subtracting the contributions from the initial state virtual photon is completely analogous [22, 23]. One calculates the  $2 \rightarrow 3$  matrix elements with  $Q^2 \neq 0$  and decomposes them into terms with the characteristic denominator from  $\gamma^* \rightarrow q\bar{q}$  splitting which become singular in the limit  $Q^2 \rightarrow 0$ . The singular terms for  $Q^2 \rightarrow 0$  of the matrix elements for transversely polarized photons after phase space integration up to a cut-off  $y_s$  have the same structure as in the real photon case. The integration can be done with  $\epsilon = 0$  since  $Q^2 \neq 0$ . In the real photon case the pole term has the form  $\frac{1}{\epsilon} P_{q\leftarrow\gamma}(z)$ , where  $P_{q\leftarrow\gamma}(z)$  is the photon to quark splitting function. Instead of the pole, for the virtual photon the logarithm

$$M = \ln \left( 1 + \frac{y_s s}{z Q^2} \right) P_{q\leftarrow\gamma}(z) \quad (16)$$

occurs, which is singular for  $Q^2 = 0$ . This singularity is absorbed into the PDF of the virtual photon with virtuality  $Q^2$ . The transition function (compare eqn (13)) reads

$$\Gamma_{q\leftarrow\gamma}^{(1)}(z, M_\gamma^2) = P_{q\leftarrow\gamma}(z) \left[ \ln \left( \frac{M_\gamma^2}{Q^2} \right) - \ln(1 - z) \right] - 1 \quad (17)$$

After absorbing  $\Gamma_{q\leftarrow\gamma}^{(1)}$  into the virtual photon PDF in analogy to eqn (12), and subtracting the logarithm from the unrenormalized cross section in analogy to eqn (14), the remaining finite term (for  $Q^2 \rightarrow 0$ ) in  $M$  yields

$$M(Q^2)_{\overline{MS}} = -P_{q\leftarrow\gamma}(z) \left[ \ln \left( \frac{M_\gamma^2 z}{z Q^2 + y_s s} \right) - \ln(1 - z) \right] + 1 \quad (18)$$

In addition to the singular term  $\ln(M_\gamma^2/Q^2)$ , two finite terms have been subtracted in order to achieve the same result as for the  $\overline{MS}$  factorization in the real photon case, when the limit  $Q^2 \rightarrow 0$  is taken in (18). Therefore this form of factorization is called the  $\overline{MS}$  factorization for  $Q^2 \neq 0$ . The term (18) is the one implemented in **JetViP** for calculating the virtual photon initial state contribution.

Taking a close look at eqn (18) one observes that it is not necessary to have a non-zero cut-off  $y_s$  to calculate the subtraction term. As long as  $Q^2 \neq 0$ , it will suffice to choose  $y_s = 0$  for evaluating the leading logarithmic contribution from the  $\gamma^* \rightarrow q\bar{q}$  splitting.

This has a numerical advantage for the comparison of the two approaches mentioned at the beginning of this section. Since  $y_s = 0$ , no cut-off is introduced in the phase space integration on the virtual photon side for the three-body direct contributions, which gives the DIS result. Thus, for comparing the two approaches, only three calculations have to be performed. After calculating the (time-consuming) DIS cross section, where  $y_s = 0$  on the virtual photon side, one can calculate the subtraction term (18) with  $y_s = 0$ , which numerically can be done very fast. Third, the resolved cross section is calculated. The approach 1 is then given by the DIS result with  $y_s = 0$ , the approach 2 is given by adding the resolved cross section and the *subtracted direct* cross section, which is obtained by adding the DIS result and the subtraction term.

However, this method can only be applied as long as  $Q^2$  is not too small. If  $Q^2$  becomes too small, the DIS cross section will start to become too large due to the logarithms  $\ln(Q^2/E_T^2)$  and the numerical integration becomes unstable and produces large statistical errors. Thus, one has to choose a finite  $y_s$  in the numerical phase space integration and in the subtraction term (18). I have observed that setting  $y_s = 0$  works well for all  $Q^2 \geq 1 \text{ GeV}^2$ . Below  $Q^2 = 1 \text{ GeV}^2$  the photoproduction regime begins and it is definitely necessary to take into account the resolved component, i.e., only approach 2 will give appropriate results. Then one has to choose a finite  $y_s$ .

In **JetViP** only the photon splitting terms for the transversely polarized photons are implemented. The longitudinal parts are proportional to  $Q^2$  and vanish in the limit  $Q^2 \rightarrow 0$ . Since they do not produce a singularity, one does not necessarily have to introduce a longitudinal virtual photon structure function. Apart from this argument, no longitudinal virtual photon structure function has been constructed so far.

## 2.4 The PDF of the Virtual Photon

The scale ( $\mu^2$ ) dependence of the parton distributions of the virtual photons with virtuality  $Q^2 \neq 0$  in the region  $\Lambda^2 \ll Q^2 \ll \mu^2$ , with  $\Lambda^2$  being a soft scale, follows from the respective evolution equations [32]. These are very similar to those for the real photon case with  $Q^2 = 0$  and contain a point-like and a hadronic part. Of special interest is the region where  $Q^2 \simeq \Lambda^2$ .

As mentioned in the introduction, mainly two different LO parametrizations of the virtual photon PDF have been constructed. These are implemented in **JetViP**. The construction is done such that the case of the real photons is reproduced for  $Q^2 \rightarrow 0$  and the exact evolution equations are obeyed for  $Q^2 \gg \Lambda^2$ :

- Glück, Reya and Stratmann (GRS) [20]: The evolution equations are solved with a smooth interpolation of the boundary conditions valid at  $Q^2 = 0$  and for  $Q^2 \gg \Lambda^2$ . LO and NLO parton distributions have been obtained in this way, but only the LO ones are parametrized in a form which is convenient for numerical calculations.

The application of the GRS PDF's is restricted to  $Q^2 \leq 10 \text{ GeV}^2$ ,  $\mu^2 \in [0.6, 5 \cdot 10^4]$

GeV<sup>2</sup> and  $Q^2 \leq 5\mu^2$ . Furthermore,  $x \in [10^{-4}, 1]$ . The number of flavours is limited to 3.

- Schuler and Sjöstrand (SaS) [17]: The dipole integral over the virtuality  $k^2 \in [0, \mu^2]$  of the  $\gamma^* \rightarrow q\bar{q}$  state is modified by the factor  $(k^2/(k^2 + Q^2))^2$ . The integration over the low  $k^2$  region,  $k^2 < \mu_0^2$ , is associated with the hadronic part, whereas the high  $k^2$  region,  $k^2 > \mu_0^2$ , is associated with the pointlike part. Different values of  $\mu_0^2$  can be selected.

The application of the SaS PDF's is not restricted kinematically, although it should be noted that in the region  $Q^2 > \mu^2$  the PDF's are nearly zero.

As a third possibility, in **JetViP** the Drees and Godbole interpolation factor is implemented:

- Drees and Godbole (DG) [19]: The quark distributions of the real photon are multiplied with the scaling factor

$$r = 1 - \frac{\ln(1 + Q^2/P_C^2)}{\ln(1 + \mu^2/P_C^2)} \quad ,$$

where  $P_C^2$  is a typical hadronic scale of order 0.5 GeV<sup>2</sup> (the value  $P_C^2 = 0.5$  GeV<sup>2</sup> is fixed in **JetViP**). The stronger suppression of the gluon distribution is modelled by multiplying these distributions with  $r^2$  instead of  $r$ .

For  $Q^2 = 0$ ,  $r = 1$  (real photon case). For  $Q^2 = \mu^2$ ,  $r = 0$  (no resolved contribution). Note, that  $r < 0$  for  $Q^2 > \mu^2$ .

In lepto-production  $E_T^2$ ,  $Q^2$  or a combination of both are possible choices for the hard scale  $\mu^2$ . In the transition region, the combination  $\mu^2 = E_T^2 + Q^2$  reproduces the scale  $E_T^2$ , used in photoproduction, in the limit  $Q^2 \rightarrow 0$ . In the DIS regime for  $Q^2 \gg E_T^2$  one has  $\mu^2 \simeq Q^2$ . Obviously, as can be seen from the restrictions of the PDF's of GRS and SaS, the choice of the scale will dramatically affect whether a resolved component is present in the theoretical calculations or not, especially in a region where  $Q^2 \simeq E_T^2$ . This is true also for the DG model. To obtain a smooth transition from the photoproduction to the DIS region, without having to bother about discontinuities on the PDF's of the resolved photon, one can choose the SaS parametrization with the scale  $\mu^2 = E_T^2 + Q^2$ , since here the restriction  $Q^2 \leq 5\mu^2$  is not built in as for the GRS parametrization. This model dependence however only reflects the fact that the structure and especially the  $Q^2$ -dependence of the virtual photon is not known well. Of course, if new parametrizations are released in the future, these will be included in **JetViP**.

It is clear that in NLO the PDF for the virtual photon must be given in the same scheme that has been used for the calculation of the  $\gamma^* \rightarrow q\bar{q}$  splitting term, i.e., the  $\overline{\text{MS}}$  factorization scheme. In [16] the PDF is constructed in the DIS <sub>$\gamma$</sub>  scheme, which is defined as

for real photons ( $Q^2 = 0$ ). This distribution function is related to the  $\overline{\text{MS}}$  scheme PDF in the following way [16]:

$$f_{a/\gamma}(x, M_\gamma^2)_{DIS_\gamma} = f_{a/\gamma}(x, M_\gamma^2)_{\overline{\text{MS}}} + \delta f_{a/\gamma}(x, M_\gamma^2) \quad (19)$$

where

$$\delta f_{q_i/\gamma}(x, M_\gamma^2) = \frac{\alpha}{2\pi} \left[ P_{q_i \leftarrow \gamma}(x) \ln \left( \frac{1-x}{x} \right) + 8x(1-x) - 1 \right] \quad (20)$$

Furthermore,  $\delta f_{q_i/\gamma} = \delta f_{\bar{q}_i/\gamma}$  and  $\delta f_{g/\gamma} = 0$ . If the PDF in this scheme is used to calculate the resolved cross section one must transform the NLO finite terms in the direct cross section. This produces a shift of  $M(Q^2)_{\overline{\text{MS}}}$  as given in (18) by the same expression as in (20). The appropriate expression has been implemented in **JetViP** to account for the  $\text{DIS}_\gamma$  scheme. Strictly speaking, the transformation (20) only makes sense for NLO PDF's. Since these are not available yet, we treat the LO parametrizations as if they were NLO. Note, that SaS have defined a slightly different  $\text{DIS}_\gamma$  scheme than GRS. The appropriate transformation formulæ for going from one scheme to the other for the SaS PDF's are not implemented in **JetViP**. However, using eqn (20) will produce results which are very similar to the correct transformation.

## 2.5 Jet Definitions

In the following I will discuss two of the main jet algorithms which are used in experiments. One is the iterative cone algorithm [33], the other is the  $k_\perp$  algorithm [34]. In both cases, a jet is defined in terms of its constituent particles. According to the Snowmass convention [29], the transverse energy  $E_{TJ}$ , pseudorapidity  $\eta_J$  and azimuth angle  $\phi_J$  of a jet are defined as

$$\begin{aligned} E_{TJ} &= \sum_i E_{T_i} \quad , \\ \eta_J &= \frac{1}{E_{TJ}} \sum_i E_{T_i} \eta_i \quad , \\ \phi_J &= \frac{1}{E_{TJ}} \sum_i E_{T_i} \phi_i \quad , \end{aligned} \quad (21)$$

where the sum runs over all partons inside the jet. The (boost-invariant) opening angle between two partons  $p_i$  and  $p_j$  in the  $(\eta, \phi)$ -plane is defined as  $R_{ij} = \sqrt{(\eta_i - \eta_j)^2 + (\phi_i - \phi_j)^2}$ .

The iterative cone algorithms, as e.g. used by the CDF and D0 collaborations, consist of the following steps [35]:

1. After particles have been clustered into calorimeter cells (CC) of certain size in  $(\eta, \phi)$ -space, each CC above a certain energy  $E_0$  is considered as a *seed cell* with direction  $(\eta_S, \phi_S)$ .

2. For each seed cell, jets are defined by summing all CC  $i$  according to eqn (21), if  $R_{iS} < R$  with a certain cone radius  $R$ . If the jet direction does not coincide with the seed direction, the seed direction is replaced by the jet direction. This step is iterated, until a stable jet direction is found.
3. All jet duplicates are thrown away.

Finally, jets which are overlapping have to be taken care of. For these, a splitting procedure is defined, which is slightly different in different experiments. In principle, jets are merged which have a certain percentage of their energy in common (typically 50% to 75%) with the direction given by the higher-energy jet, and split otherwise.

In **JetViP**, partons are combined into a jet with direction  $(\eta_J, \phi_J)$  also according to eqn (21). A parton  $p_i$  is included into the jet, if the condition

$$\sqrt{(\eta_i - \eta_J)^2 + (\phi_i - \phi_J)^2} < R \quad (22)$$

is fulfilled, where  $R$  is the same as in step 2 in the above procedure. This definition is analogous to combining two partons  $p_i$  and  $p_j$  into a single jet, if they fulfill the condition

$$R_{ij} \leq R \cdot E_{ij} \quad \text{with} \quad E_{ij} \equiv \frac{E_{T_i} + E_{T_j}}{\max(E_{T_i}, E_{T_j})} \quad (23)$$

This kind of parton level jet definition is very similar to the steps 1–3 in the above described algorithm. Since at NLO we have at most three partons in the final state, the theoretical procedure is of course much simpler. There are no iterations needed to define stable jets and at maximum only two partons can be merged in the hadronic c.m.s. due to momentum conservation. Finally, no merging or splitting of two clusters depending on their shared energy occurs.

There is, however, a well-known problem for iterative cone algorithms [35]. It arises from configurations, where particles with balanced  $E_T$  have a distance between  $R$  and  $2R$ , so that both particles are within  $R$  of their common center, see Fig. 2 (a). For this configuration, the iterative cone algorithm will produce two stable jets since no other particle is in the intermediate region.

This situation does not change if an additional soft particle below the threshold  $E_0$  is added in the center between particles  $p_i$  and  $p_j$ , see Fig. 2 (b). However, if the third particle is slightly above the threshold, it will be considered as an additional seed cell. Since the cone around the seed encloses the other two particles, all three particles will be merged into a single stable jet, in contrast to the two-jet configuration without an additional soft particle. It is clear that the so found cross sections depends on the energy threshold  $E_0$ . Thus, the iterative cone algorithm is not fully infrared safe. Furthermore, if the soft particle above  $E_0$  splits into two collinear particles slightly below  $E_0$  in two slightly different CC, the single-jet configuration will flip back to a two-jet one. So the iterative cone algorithm is also not fully collinear safe.

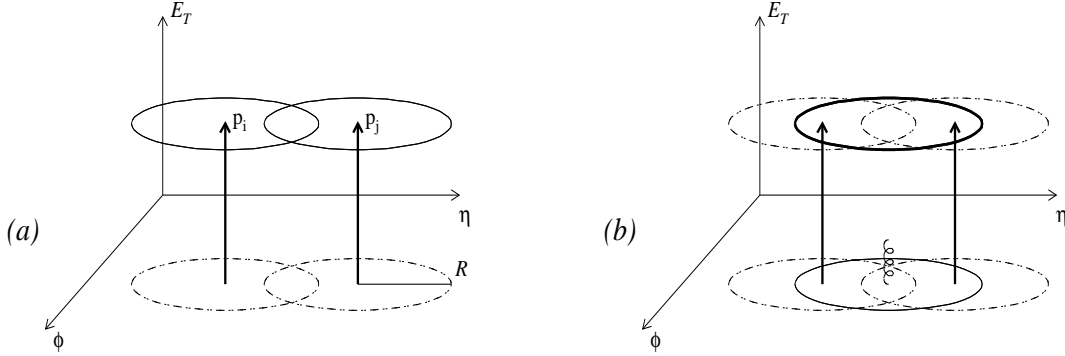


**Figure 2:** (a) Two partons  $p_i$  and  $p_j$  in the  $(\eta, \phi)$ -plane with a distance between  $R$  and  $2R$  with balanced  $E_T$ . (b) Additional soft particle in the overlap region (figure adapted from [35]).

At NLO, this behaviour can not be observed, since there are no soft particles available. To simulate the overlap problem in the theoretical analysis in a simple way, Ellis, Kunszt and Soper have introduced the concept of the phenomenological  $R_{sep}$  parameter [36]. EKS suggested to imply the constraint, that the distance between the two partons should not only fulfill eqn (23), but also be less than  $R_{sep}$ . Thus, two partons  $p_i$  and  $p_j$  are combined into a single jet, if the condition  $R_{ij} \leq \min(R \cdot E_{ij}, R_{sep})$  is fulfilled.

A number of objections can be raised against this kind of solution, which have been discussed in [35]. A jet definition that avoids all the discussed problems is the  $k_\perp$  algorithm. Including an  $R$  parameter the steps in the experimental analysis are [34]:

1. For every pair of particles, define a closeness  $d_{ij} = \min(E_{T_i}, E_{T_j})^2 R_{ij}^2$  (for small opening angles  $R_{ij} \ll 1$ , one finds  $d_{ij} \simeq \min(E_i, E_j)^2 \theta_{ij}^2 \simeq k_\perp^2$ ).
2. For every particle define a closeness to the beam particles  $d_{iB} = E_{T_i}^2 R^2$ .
3. If  $\min(d_{ij}) < \min(d_{iB})$ , merge particles  $p_i$  and  $p_j$  according to eqn (21). If otherwise  $\min(d_{ij}) > \min(d_{iB})$ , jet  $i$  is complete.

These steps are iterated until all jets are complete. As a result, all jets are at least  $R$  apart and all opening angles within each jet are less than  $R$ . The NLO calculation produces jets equal to those found in the  $k_\perp$  algorithm by combining two particles  $p_i$  and  $p_j$  according to eqn (21), if they fulfill the condition  $R_{ij} < R$ , that is by choosing the  $R_{sep}$  modified cone algorithm with  $R_{sep} = R$  (since  $E_{ij} \geq 1$ ).

### 3 Jet Cross Sections in Photon-Photon Scattering

We will now extend the case of  $eP$ -scattering to include the scattering of virtual on real photons, as it can be achieved at  $e^+e^-$  colliders.



### 3.1 General Structure of Cross Sections

To fix the notation we start by writing down the process of jet production in  $e^+e^-$  scattering:

$$e^+(k_a) + e^-(k_b) \longrightarrow e^+(k'_a) + e^-(k'_b) + \text{jet}_1(E_{T_1}, \eta_1) + \text{jet}_2(E_{T_2}, \eta_2) + X \quad . \quad (24)$$

We are interested in the case where one lepton radiates a virtual and the other a real photon. Of course, it does not matter which of the leptons radiates the virtual photon, but for definiteness we suppose this to be the positron. Thus, the subprocess we have to consider is  $\gamma_a^*(q_a) + \gamma_b(q_b) \rightarrow \text{jet}_1 + \text{jet}_2 + X$ , with  $q_a = k_a - k'_a$ ,  $q_b = k_b - k'_b$  and the virtualities  $Q^2 = -q_a^2$  and  $P^2 = -q_b^2 = 0$ . The electron-positron center-of-mass energy is  $s_H = (k_a + k_b)^2$ . The energy in the hadronic, i.e.,  $\gamma^*\gamma$ , c.m.s. is  $W^2 = (q_a + q_b)^2$ . Furthermore we define the variables

$$y_a = \frac{q_a k_b}{k_a k_b} \quad \text{and} \quad y_b = \frac{q_b k_a}{k_a k_b} \simeq 1 - \frac{E'_e}{E_e} \quad , \quad (25)$$

where  $E_e$  and  $E'_e$  are the energies of the incoming and outgoing electron in the  $e^+e^-$  c.m.s., respectively. The variable  $y_b$  gives the momentum fraction of the real photon in the electron.

As for  $eP$ -scattering, the virtual photon can have a point-like part and a non-perturbative, resolved structure for moderate  $Q^2$ . The point-like and hadronic components are likewise found for the real photon with  $P^2 = 0$ . Taking all possible interaction modes into account, one finds in total four contributions for the interaction of real and virtual photons (see Fig. 3):

1. Direct (D): both photons couple directly to the charge of the quarks.
2. Single-resolved (SR): the real photon is resolved and the virtual photon interacts directly with the partons from the photon.
3. Single-virtual-resolved (SR\*): the virtual photon is resolved and the real photon interacts directly with the partons from the virtual photon.
4. Double-resolved (DR): both photons are resolved.

The contributions 2 and 4 are familiar from  $eP$ -scattering with the resolved photon substituted by a proton and thus have a structure very similar to that encountered in DIS. The subprocesses for these contributions are listed in Tab. 1 and 2. The subprocesses of contribution 3 are easily obtained from contribution 2 by setting  $Q^2 = 0$ . Contribution 1 has no counterpart in  $eP$ -scattering and has been calculated in NLO QCD in [27]. It consists in LO of the Born process  $\gamma^*\gamma \rightarrow q\bar{q}$  and in NLO of the one-loop corrections to the Born process and the real gluon emission process  $\gamma^*\gamma \rightarrow q\bar{q}g$ . This completes the list of processes implemented in **JetViPas** given in Tab. 1 and 2.

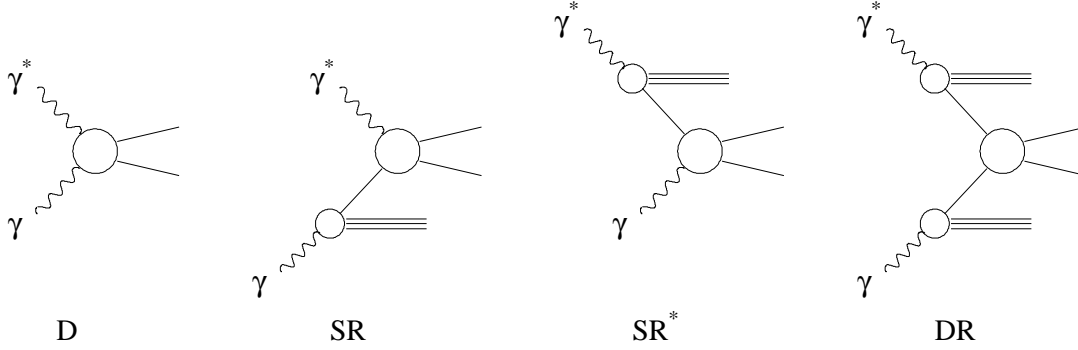


**Figure 3:** The different components contributing in  $\gamma^*\gamma$  scattering.

Taking into account both the transverse and longitudinal polarizations of the virtual photon, the cross section  $d\sigma_{e^+e^-}$  for the processes 1–4 is conveniently written as the convolution

$$\begin{aligned} \frac{d\sigma_{e^+e^-}}{dQ^2 dy_a dy_b} &= \sum_{a,b} \int dx_a dx_b F_{\gamma/e^-}(y_b) f_{b/\gamma}(x_b) d\sigma_{ab} \\ &\times \frac{\alpha}{2\pi Q^2} \left[ \frac{1 + (1 - y_a)^2}{y_a} f_{a/\gamma^*}^U(x_a) + \frac{2(1 - y_a)}{y_a} f_{a/\gamma^*}^L(x_a) \right] . \end{aligned} \quad (26)$$

The PDF's of the real and the virtual photon are  $f_{b/\gamma}(x_b)$  and  $f_{a/\gamma^*}^{U,L}(x_a)$ , respectively. The direct processes are included in formula (26) through delta functions. For the direct virtual photon one has  $f_{a/\gamma^*}^{U,L} d\sigma_{ab} = \delta(1 - x_a) d\sigma_{\gamma^* b}^{U,L}$ , whereas for the direct real photon the relation is  $f_{a/\gamma} d\sigma_{ab} = \delta(1 - x_b) d\sigma_{\gamma b}$ . As for the  $eP$  process, only the unpolarized PDF  $f_{a/\gamma}^U$  is implemented in **JetViP**, because the subtraction procedure has only been worked out for that case.

The function  $F_{\gamma/e^-}(y_b)$  describes the spectrum of the real photons emitted from the electron according to the Weizsäcker-Williams approximation [37], which in its' simplest form reads

$$F_{\gamma/e^-}(y_b) = \frac{\alpha}{2\pi} \frac{1 + (1 - y_b)^2}{y_b} \ln \left( \frac{E_e^2 \theta_{max}^2}{m_e^2} \right) . \quad (27)$$

The electron mass is  $m_e$  and  $\theta_{max}$  is the maximum scattering angle of the electron.

All other aspects of jet cross sections that have been addressed in the connection with  $eP$ -scattering, as there are the subtraction of virtual photon initial state singularities, the virtual photon structure function, or the jet algorithms, remain unchanged for  $\gamma^*\gamma$  reactions. The frame of reference in which cross sections are calculated is the hadronic (i.e.,  $\gamma^*\gamma$ ) c.m.s.

### 3.2 Notation of Subprocesses in JetViP

As we have seen, the  $\gamma^*\gamma$  reactions and the  $eP$  processes have quite a number of subprocesses in common. To unify the notation and to therefore simplify the handling of the input-file, which will be described in the following section, we will denote the direct process in  $eP$ -scattering as SR, whereas the resolved contribution is denoted as DR.

## 4 Definition and Range of Input Parameters

Now that the theoretical concepts underlying the program have been clarified, we turn our attention to the details of setting the parameters in the input-file to obtain a jet cross section from **JetViP**. The input-file needs to have the exact format as shown in appendix A (the file shown in the appendix contains a set of standard values to produce a single-jet inclusive LO cross section in  $eP$ -scattering for HERA conditions). The input-file has five main categories, which are:

1. Specification of the process and contributions to the process.
2. Specification of the initial state (of the real and virtual photons and/or proton). This includes the energies of the incoming particles and the kinematics of the incoming and outgoing leptons.
3. Specification of the kinematics and parameters relevant for calculating the subprocess. This includes the specification of the parton densities for the photon and/or proton and of the scales.
4. Specification of the final state jets.
5. Specification of the parameters for the **VEGAS** integration routine.

In the following, the definition and range of the parameters occurring in these categories will be explained. Numbers in squared brackets point to the section where the relevant theoretical concept is discussed.

### 4.1 Contribution

- **iproc**: integer  $\in \{1, 2\}$ . Type of process. 1 =  $eP$ , 2 =  $e^+e^-$
- **ijet**: integer  $\in \{1, 2\}$ . 1 = single-jet, 2 = dijet.
- **isdr**: integer  $\in \{1, 2, 3, 4\}$ . Selection of the D, SR, SR\* or DR contribution. [sec 3.2] 1 =D; 2 =SR; 3 =SR\*; 4 =DR. Only one of the contributions D, SR, SR\* or DR can be calculated at a time. They have to be added after the calculation.

In the following, the LO and NLO contributions are turned on (1) or off (0):

- **iborn**: integer  $\in \{0, 1\}$ . Born process ( $2 \rightarrow 2$ ).
- **ivirt**: integer  $\in \{0, 1\}$ . Virtual correction ( $2 \rightarrow 2$ ).
- **ifina**: integer  $\in \{0, 1\}$ . Final state singularities ( $2 \rightarrow 2$ ).
- **iaini**: integer  $\in \{0, 1\}$ . Initial state singularities on side  $a$ , i.e., the virtual photon side ( $2 \rightarrow 2$ ). For calculating a DIS (direct) cross section, **iaini**= 0 and **iqcut**= 0 (see below), since no initial state singularity for the virtual photon has to be subtracted. For the D and SR contributions, **iaini** has to be calculated separately, due to different kinematics than the other  $2 \rightarrow 2$  processes. In photoproduction and for the DR contributions, set **iaini**= 1 with a finite value of **cutmin** (see below). For calculating the virtual photon splitting term in DIS, calculate **iaini** separately with **cutmin**= 0.00 (see below). [sec 2.3]
- **ibini**: integer  $\in \{0, 1\}$ . Initial state singularities on side  $b$  ( $2 \rightarrow 2$ ), i.e., for the real photon or the hadron, according to **iproc**.
- **iinco**: integer  $\in \{0, 1\}$ . NLO  $2 \rightarrow 3$  contribution inside jet cone. Setting  $R = 0$  (see below) will suppress these contributions.
- **iouco**: integer  $\in \{0, 1\}$ . NLO  $2 \rightarrow 3$  contribution outside jet cone.

For a LO calculation, only **iborn**= 1. For a complete NLO calculation, all parameters **iborn**, **ivirt**, ..., **iouco** have to be set equal to 1 (modulo the changes for DIS or photoproduction cross sections or for calculating the  $\gamma^* \rightarrow q\bar{q}$  subtraction term).

- **iqcut**: integer  $\in \{0, 1\}$ . Insert a finite cut-off  $y_s$  (**cutmin**) into the integration on the virtual photon side for the  $2 \rightarrow 3$  NLO contributions ( $= 1$ ) or not ( $= 0$ ). See remarks for **iaini**. [sec 2.3]

## 4.2 Initial State

- **Ea**, **Eb**: real\*8. Energies of the incoming particles  $a$  and  $b$  in GeV. Particle  $a$  is always the lepton on the virtual photon side, whereas particle  $b$  is a hadron for **iproc**= 1 and a lepton for **iproc**= 2.
- **iframe**: integer  $\in \{0, 1\}$ . Defines the frame of reference, in which the cross sections are calculated. Setting **iframe** = 0 selects the hadronic c.m.s. Setting **iframe** = 1 selects the laboratory frame (only correct for photoproduction, i.e.,  $Q^2 \lesssim 1 \text{ GeV}^2$ ).
- **izaxis**: integer  $\in \{-1, 1\}$ . Defines the direction of the incoming electron. For **izaxis**= 1 the electron is traveling in the positive  $z$ -direction, for **izaxis**= -1 it is traveling into the negative  $z$ -direction.

- **iQ2**: integer  $\in \{0, 1, 2, 3, \dots\}$ . For **iQ2**= 0,  $Q^2$  is integrated in [**Q2min**, **Q2max**]. For **iQ2**= 1,  $d\sigma/dQ^2$  is calculated at **Q2min**. For **iQ2**> 1,  $d\sigma/dQ^2$  is calculated at  $n = \text{iQ2}$  equidistant  $Q^2$  points in [**Q2min**, **Q2max**].
- **Q2min**, **Q2max**: real\*8  $\geq 0$ . Minimum and maximum value of  $Q^2$ . Setting **Q2min** = 0 will produce a photoproduction cross section. Remember setting **iqcut**= 1 for photoproduction cross sections.
- **iypol**: integer  $\in \{1, 2, 3\}$ . Polarization of the virtual photon.  
1 = transverse (T), 2 = longitudinal (L), 3 =T+L.

### 4.3 Subprocess

- **W2min**: real\*8. Minimum value of hadronic c.m.s. energy.
- **xhmin**, **xhmax**: real\*8  $\in [0, 1]$ . Minimum and maximum value of  $x_{Bj}$ .
- **Nf**: real\*8  $\in \{1, 2, 3, 4, 5\}$ . Number of active flavours.
- **lambda**: real\*8 > 0 in GeV. Value of  $\Lambda_{QCD}$  for **Nf** flavours.
- **ialphas**: integer  $\in \{1, 2\}$ . One-loop (**ialphas**= 1) or two-loop (**ialphas**= 2) formula for the strong coupling constant  $\alpha_s$  without thresholds. For **ialphas** = 3 the value of  $\alpha_s$  is taken from the PDFLIB (automatically adjusts  $\Lambda$ ).
- **icut**: integer  $\in \{1, 2, 3, \dots\}$ . Phase space slicing parameter  $y_s$ . For **icut**= 1,  $y_s$  is set equal to **cutmin**. For **icut**> 1, the cross section will be calculated at  $n = \text{icut}$  points with logarithmic spacing in the range [**cutmin**, **cutmax**].
- **cutmin**, **cutmax**: real\*8 > 0. Minimum and maximum value of  $y_s$ . The independence of the NLO cross sections on  $y_s$  has been tested for  $y_s \in [10^{-2}, 10^{-4}]$ . Large statistical errors occur for too small  $y_s$ . Recommended value:  $y_s = 10^{-3}$ .
- **fproc**: integer  $\in \{1, 2, 3\}$ . Selection of partons from PDF's. 1 =gluon, 2 =quarks, 3 =  $q + g$ .
- **idisga**: integer  $\in [0, 1]$ . Since all partonic cross sections in **JetViP** are implemented in the  $\overline{\text{MS}}$ -scheme, a photon PDF constructed in the  $\text{DIS}_\gamma$  scheme has to be transformed into the  $\overline{\text{MS}}$ -scheme. This is done for the photon on side a by setting **idisga**= 1. [sec 2.4, page 14]
- **xaobsmn**, **xaobsmx**: real\*8  $\in [0, 1]$ . Minimum and maximum value of  $x_\gamma^{obs}$  for the virtual photon.
- **ipdftyp**: integer  $\in \{1, 2, 3, 4\}$ . Selects the PDF for the resolved virtual photon.  
1 = SaS, 2 = GRS, 3 = DG, 4 = PDFLIB (for real photons with  $Q^2 = 0$ ).

- **igroupa**: integer. For **ipdftyp**= 3,4 this selects the group from the PDFLIB (see manual [38]). For **ipdftyp**= 1 this represents **isasset**  $\in \{1, 2, 3, 4\}$ , which selects input scale and scheme of SaS virtual photon PDF (see [17]).
- **iseta**: integer. For **ipdftyp**= 3,4 this selects the set from the PDFLIB (see manual [38]). For **ipdftyp**= 1 this represents **isasp2**  $\in \{1, 2, 3, 4, 5, 6, 7\}$ , which selects the scheme used to evaluate off-shell anomalous component in SaS virtual photon PDF (see [17]).
- **idisgb**: integer  $\in \{0, 1\}$ . See **idisga**.
- **xbobsmn**, **xbobsmx**: real\*8  $\in [0, 1]$ . Minimum and maximum value of  $x_\gamma^{obs}$  for real photon (only in  $e\gamma$ -scattering). [not yet implemented!]
- **igroupb**: integer. Selects the group from PDFLIB for the resolved component for particle b (see manual [38]). **iproc** automatically selects, if a hadron or a photon PDF is used.
- **isetb**: integer. Selects the set from PDFLIB (see manual [38]).
- **a**, **b**, **c**: real\*8  $> 0$ . Choosing the overall-scale  $\mu^2$  according to  $\mu^2 = a + bQ^2 + cp_T^2$ .

## 4.4 Final State

- **jr**: real\*8  $\geq 0$ . Jetradius for cone algorithm. [sec 2.5]  
By setting **jr**= 0, the function **kincut** (see below) gives the kinematic variables of the partons, rather than those of the jets. Thus, other jet recombination schemes, apart from the cone algorithms, can be implemented.
- **Rsep**: real\*8  $> 0$ . The  $R_{sep}$  parameter for the modified Snowmass cone algorithm. Setting  $R_{sep} = R$  (i.e. **jr**=**Rsep**) selects the  $k_\perp$  algorithm. [sec 2.5]

The following variables are the  $E_T$ 's and  $\eta$ 's of the final state jets. The final state phase space  $dPS^{(n)}$  is parametrized by these variables, so that a restriction on the  $E_T$ 's and  $\eta$ 's does not reduce the statistics. All VEGAS-points are thrown inside the given limits. If the limits are outside the physical ranges, the program will automatically set the physically possible limits for the variables, as they follow from energy-momentum conservation. The terminology is the same as used for **iQ2**, **Q2min**, **Q2max**:

- **ipt**: integer  $\in \{0, 1, 2, 3, \dots\}$ . Transverse energy  $E_{T_1}$  of the trigger jet. This is not necessarily the hardest jet. The transverse energy of the second jet  $E_{T_2}$  is accessible in the user defined routine **kincut** (see below).
- **ptmin**, **ptmax**: real\*8  $> 0$ . Minimum and maximum value of  $E_{T_1}$ .

- **ieta1**: integer  $\in \{0, 1, 2, 3, \dots\}$ . Rapidity  $\eta_1$  of the trigger jet.
- **etamin1**, **etamax1**: real\*8  $> 0$ . Minimum and maximum value of  $\eta_1$ .
- **ieta2**: integer  $\in \{0, 1, 2, 3, \dots\}$ . Rapidity  $\eta_2$  of the second jet.
- **etamin2**, **etamax2**: real\*8  $> 0$ . Minimum and maximum value of  $\eta_2$ .

## 4.5 Vegas and Output

- **ipoint**: integer  $> 0$ . Defines the statistics of the integration. Typical value for LO: **ipoint** = 3000. Gives accuracy of under 1%. Typical value for NLO direct **ipoint** = 100000, for NLO resolved **ipoint** = 150000. Gives accuracy of around 3% (the accuracy also depends on the selected value of the slicing parameter  $y_s$ . For smaller  $y_s$ , larger compensations occur and therefore the statistical errors become larger).
- **itt**: integer  $> 0$ . Number of iterations for **Vegas**. Recommended value: **itt**= 5.
- **iprn**: integer  $\in \{0, 10\}$ . For **iprn** = 0, no output will be given. For **iprn** = 10, the result of the iterations of **Vegas** will be printed on the screen.
- **eps**: integer  $> 0$ . Precision of the **Vegas** integration. Recommended value: **eps**= $10^{-5}$ .
- **jfileout**: character\*20. Name of the output-file.

## 4.6 The User-defined Function kincut

To allow a high flexibility for incorporating specific types of jet selection processes and kinematic cuts, characterizing certain experiments, the user can edit the function **kincut.f**. The following variables are **common** and therefore accessible by the user:

**y, x-bj, Q2, sH, elek, prot, Nc, Cf, pi, me**

The jet-variables  $E_T$ ,  $\eta$  and  $\phi$ , are stored in the three-dimensional vectors **jet1(i)**, **jet2(i)** and **jet3(i)** for  $i=1,2,3$ . The first entry of each vector gives the transverse energy, the second gives the rapidity and the third gives the azimuthal angle. If there are only two jets in the final state, the vector **jet3** contains the value  $-10^5$  in each entry. Note, that the first and second jet are not ordered in  $E_T$ . However, the transverse energy of the third jet is always smaller than the transverse energy of the other two,  $E_{T_3} < \min(E_{T_1}, E_{T_2})$ .

If the kinematic cuts are passed, **kincut** returns 0, otherwise 1.

## 5 Using JetViP on Computers

### 5.1 Environment and Installation

JetViP is programmed in standard FORTRAN 77. The multidimensional phase-space integration is performed with help of the Vegas [31] Monte-Carlo integration routine. Further packages used are the PDFLIB, SaSGAM and GRS PDF's.

The JetViP package is accessible via [www](http://www.desy.de/~poetter/jetvip.html).<sup>2</sup> The source-code has been translated and tested for the HP-UX, IRIX (SGI) and Linux computing platforms. Other platforms can be made available upon request from the author. The package is tarred and can be installed by doing `tar xf name.tar`. It contains the following files:

- Makefile: Typing `make` will produce an executable JetVIP. Check the Makefile to make sure, the path for the PDFLIB's is correct (the standard path is `/cern/pro/lib`).
- common.f: Contains all common variables.
- jv-master.o: The object-file of the main program JetViP.
- kincut.f: A function, where the user can implement specific cuts on jet variables.
- libVegas-\$ARCH.a: The Vegas library, containing the Monte-Carlo integration routine for the architecture ARCH.
- st.in: An example of the input-file. It will produce a LO calculation of the  $E_T$ -spectrum of the direct reaction for  $eP$ -scattering at HERA. The results are written to the output-file `test.out`.

For running JetViP with the example file, type `JetVIP st.in [return]`.

### 5.2 Typical Running Times

The running times for LO and NLO calculations are very different. If we start with a LO calculation, the benchmarks listed in Tab. 3 exist for different machines (as an example calculation we have chosen the steering file shown in the appendix, which calculates the SR component). When the DR processes are considered, the running times are typically 3–4 times longer.

In a NLO calculation, the two-body and three-body processes are calculated separately. The two-body processes are large and negative and the three-body processes large and positive. Therefore, adding both contributions to have the result will produce large compensations between the two components. The statistical error from the Vegas integration,

---

<sup>2</sup>The [www](http://www.desy.de/~poetter/jetvip.html)-page is: <http://www.desy.de/~poetter/jetvip.html>.



Table 3: Benchmarks for a DIS calculation at HERA in LO with JetViP.

<b>HP-UX</b> (translated on HP-UX9)	HP-UX9	19.1 s
	HP-UX10	14.0–24.2 s
<b>IRIX</b> (translated on IRIX5.3)	IRIX5.3	63.8 s
	IRIX6.2	38.1 s
<b>Linux</b> (translated on Pentium II)	133MHz	40.8 s
	333 MHz	11.6 s

which is small for each component alone, is then large compared to the sum of the two components. Therefore, the parameter `ipoint` in the steering file has to be a factor of 50 larger for a NLO calculation, than for LO calculation, which makes the NLO calculation rather slow.

Typically, calculating a NLO SR cross section with fixed bin-size in one of the kinematical variables will take around 30 minutes. The DR contributions will take from 2 to 4 hours, due to the large number of matrix elements that have to be considered in the calculation.

## Acknowledgments

I have profited very much from discussions with D. Graudenz, M. Klasen, T. Kleinwort and G. Kramer. I thank T. Kleinwort for the consent in using his implementation of the resolved-resolved matrix elements and for his support concerning technical questions of the computing environment. Several comments from users have improved the code of the program. In particular I am grateful to S. Mattingley, T. McMahon, M. Tasevsky, J.H. Vossebeld and M. Wobisch. I thank G. Kramer for comments on the manuscript.

## References

- [1] I. Abt et al., H1 Collaboration, Phys. Lett. B314 (1993) 436; T. Ahmed et al., H1 Collaboration, Phys. Lett. B297 (1992) 205; Phys. Lett. B299 (1993) 37; S. Aid et al., H1 Collaboration, Z. Phys. C70 (1996) 17.
- [2] M. Derrick et al., ZEUS Collaboration, Phys. Lett. B297 (1992) 404; Phys. Lett. B322 (1994) 287; Phys. Lett B342 (1995) 417; Phys. Lett. B348 (1995) 665.
- [3] ZEUS Collaboration, Contribution to the XXVIII ICHEP, Warsaw, July 1996, pa02-040.
- [4] H1 Collaboration, Phys. Lett. B299 (1993) 385; Phys. Lett. B298 (1993) 469.
- [5] ZEUS Collaboration, Phys. Lett. B303 (1993) 183; Phys. Lett. B306 (1993) 158.
- [6] M. Klasen, G. Kramer Z. Phys. C72 (1996) 107; M. Klasen report DESY 96-204 (thesis); M. Klasen, T. Kleinwort, G. Kramer, EPJdirect C1 (1998) 1.
- [7] B.W. Harris, J.F. Owens, Phys. Rev. D57 (1998) 5555.
- [8] P. Aurenche, L. Bourhis, M. Fontannaz, J.P. Guilett, Proc. of "Future Physics at HERA", Hamburg, 1996 and L. Bourhis, Proceedings of the QCD Workshop, Moriond 1998.
- [9] T. Brodtkorb, J.G. Körner, E. Mirkes, G.A. Schuler, Z. Phys. C44 (1989) 415; E. Mirkes, D. Zeppenfeld, Phys. Lett. B380 (1996) 23; Acta Phys. Polon. B27 (1996) 1392; E. Mirkes, report TTP97-39 [hep-ph/9711224].
- [10] D. Graudenz, Phys. Rev D49 (1994) 3291; Phys. Lett. B256 (1992) 518.
- [11] S. Frixione, Nucl. Phys. B507 (1997), 295; S. Frixione, G. Ridolfi, Nucl. Phys. B507 (1997) 315.
- [12] S. Catani, M. Seymour, Nucl. Phys. B485 (1997) 291, Phys. Lett. B378 (1996) 287; Proceedings of the 'Workshop on Future Physics at HERA', Vol. 1 (1996) 519 [hep-ph/9609521].
- [13] D. Graudenz, Proceedings of the Workshop 'New Trends in HERA Physics', report PSI-PR-97-20 [hep-ph/9709240].
- [14] M.L. Utley (ZEUS collaboration), Univ. Glasgow report GLAS-PPE/95-03, talk given at EPS Conference, Brussels, 1995, [hep-ph/9508016]; C. Foudas (ZEUS collaboration), talk given at DIS96 Workshop, Rome, 1996;
- [15] C. Adloff et al. (H1 Collaboration), Phys. Lett. B415 (1997) 418; T. Ebert (H1 Collaboration), talk given at the DIS96 Workshop, Rome, 1996; M. Wobisch (H1 Collaboration), talk given at DIS98 Workshop, Brussels, 1998.

- [16] M. Glück, E. Reya, M. Stratmann, Phys. Rev. D51 (1995) 3220.
- [17] G.A. Schuler, T. Sjöstrand, Z. Phys. C68 (1995) 607; Phys. Lett. B 376 (1996) 193.
- [18] Ch. Berger et al., PLUTO Collaboration, Phys. Lett. B142 (1984) 119.
- [19] M. Drees, R.M. Godbole, Phys. Rev. D50 (1994) 3124.
- [20] M. Glück, E. Reya, M. Stratmann, Phys. Rev. D54 (1996) 5515.
- [21] D. de Florian, C. Garcia Canal, R. Sassot, Z. Phys. C75 (1997) 265; J. Chyla, J. Cvach, proceeding of the Workshop 1995/96 on 'Future Physics at HERA', eds. G. Ingelman, A. de Roeck, R. Klanner, DESY 1996, Vol. 1, p. 545.
- [22] M. Klasen, G. Kramer, B. Pötter, Eur. Phys. J. C1 (1998) 261.
- [23] B. Pötter, report DESY 97-138 (thesis) [hep-ph/9707319].
- [24] G. Kramer, B. Pötter, report DESY 98-046 [hep-ph/9804352].
- [25] Report on " $\gamma\gamma$  Physics", conveners P. Aurenche and G.A. Schuler, to appear in the proceedings of the 1995 LEP2 Physics workshop [hep-ph/96101317].
- [26] Report of the working group on two photon physics at Phenomenology Workshop on LEP2 Physics, Oxford, 14-18 April 1997, conveners S. Cartwright, M.H. Seymour, J.Phys. G24 (1998) 457.
- [27] B. Pötter, report DESY 98-052 [hep-ph/9805436].
- [28] D. Graudenz, DISASTER++, Version 1.0 [hep-ph/9710244].
- [29] J.E. Huth et al., Proc. of the 1990 DPF Summer Study on High Energy Physics, Snowmass, Colorado, edited by E.L. Berger, World Scientific, Singapore, 1992, p. 134.
- [30] B. Pötter, Proceedings of the 6th International Workshop on Deep Inelastic Scattering and QCD, 04-08 April 1998, Brussels.
- [31] G.P. Lepage, J. Comp. Phys. 27 (1978) 192.
- [32] C.T. Hill, G.G. Ross, Nucl. Phys. B148 (1979) 373; T. Uematsu, T.F. Walsch, Phys. Lett. B101 (1981) 263; Nucl. Phys. B199 (1982) 93.
- [33] F. Abe et. al. (CDF Collaboration), Phys. Rev. D45 (1992) 1448.
- [34] S. Catani, Yu.L. Dokshitzer, M.H. Seymour, B.R. Webber, Nucl. Phys. B406 (1993) 187.
- [35] M.H. Seymour, Nucl.Phys. B513 (1998) 269.

- [36] S.D. Ellis, Z. Kunszt, D.E. Soper, Phys. Rev. Lett. 69 (1992) 3615.
- [37] C.F. v. Weizsäcker, Z. Phys. 88 (1934) 612; E.J. Williams, Kgl. Danske Vidensk. Selskab. Mat-Fiz. Medd. 13 (1935) N4.
- [38] H. Plochow-Besch, PDFLIB User's Manual, Version 4.17 (1994); Comp. Phys. Comm. 75 (1993) 396.

## Appendix A: Input-file

The following example of an input file will produce an  $E_T$  spectrum of the direct component of the single-jet cross section  $d\sigma/dE_T$  in  $eP$ -collisions under typical HERA conditions in LO in the hadronic c.m.s., using the scale  $\mu^2 = Q^2 + E_T^2$ .

```

=====
'
      CONTRIBUTION
'
=====
1      iproc      [1=ep; 2=ee]
1      ijet       [1=Single Jet; 2=Dijet]
2      isdr       [1=D; 2=SR; 3=SR*; 4=DR]
1      iborn      [born]
0      ivirt      [virtual]
0      ifina      [final state sing.]
0      iaini      [initial state sing. side a]
0      ibini      [initial state sing. side b]
0      iinco      [2-->3 inside cone]
0      iouco      [2-->3 outside cone]
0      iqcut      [yqi-min in 2->3 matrices? 1=yes; 0=no]
=====
'
      INITIAL STATE
'
=====
27.5d0  Ea        [energy on side a (ep,ee: lepton)]
820.d0  Eb        [energy on side b (ep: proton; ee: lepton)]
'----- Frame of reference -----
0      iframe     [frame of ref: 0=hadr CMS; 1=HERA-Lab]
1      izaxis     [lepton "a" travels in pos (=1) or neg (= -1) z-dir]
'----- Lepton a -----
0      iQ2        [0=si; 1=dsi/dQ2; >1=dsi/dQ2(Q2)]
5.d0    Q2min     [0.d0 selects photoproduction]
11.d0   Q2max
0      iwwa       [which Weizs.-Will.: 0=ln(Q2mx/Q2mn); 1=ln(thmax/me)]
0.d0    thetamn   [min angle of deflection for lepton in DIS]
180.d0  thetamx   [max angle]
11.d0   Ea-min'   [min energy of outgoing lepton]
0.05d0  ymin      [min y]
0.6d0   ymax      [max y]
3      iypol      [Photon polarization: 1=T, 2=L, 3=L+T]
'----- Lepton b (only relevant for the ee-case ) -----
4.d0    P2max     [P2=virtuality of real photon]
0      iwwb       [which Weizs.-Will.: 0=ln(P2mx/P2mn); 1=ln(thmax/me)]
180.d0  thetbmx   [max angle for Weizs.-Will]

```

```

'=====
'      SUBPROCESS'
'=====
0.d0      W2min      [min hadronic cms energy]
0.d0      xhmin      [min x-bjorken]
1.d0      xhmax      [max x-bjorken]
5.d0      Nf         [Number of active flavours]
0.204d0   lambda     [Lambda-QCD (has to match Nf)]
2         ialphas    [QCD coupling: 1=one-loop; 2=two-loop; 3=PDFLIB]
1         icut       [Slicing param. y-cut: 1=fixed; >1=si(y-cut)]
1.d-3     cutmin
1.d-3     cutmax
'----- PDFs for the resolved contributions -----
3         fproc      [Parton from PDF: 1=g, 2=q, 3=q+g]
0         idisga     [DISg -> MSbar for photon a]
0.d0      xaobsmn    [photon a - minimal xa-gamma obs]
1.d0      xaobsmx    [max xa-gamma obs]
1         ipdftyp    [PDF for y*(res): 1=SaS; 2=GRS; 3=DG; 4=PDFLIB]
1         igroupa    (Param. for SaS or PDFLIB --> see manual)
2         iseta      ( " )
1         idgsas     ( " )
0.d0      xbobsmn    [photon b - minimal xb-gamma obs]
1.d0      xbobsmx    [max xb-gamma obs]
4         igroupb    [authors of PDF on side b: y(res) or prot]
34        isetb      [Set-No]
'----- Scales -----
0.d0      a          [Scale: mu**2=a+b*Q**2+c*pt**2]
1.d0      b
1.d0      c
'=====
'      FINAL STATE'
'=====
1.d0      jr         [Jetradius for Snowmass convention]
2.d0      Rsep       [R-sep parameter]
'----- Jet variables -----
11        ipt        [0=si; 1=dsi/dpt; >1=dsi/dpt(pt)]
5.d0      ptmin      [pt of trigger jet]
15.d0     ptmax
0         ieta1       [0=si; 1=dsi/deta1; >1=dsi/deta1(eta1)]
-30.d0    eta1min     [eta of trigger jet]
30.d0     eta1max
0         ieta2       [0=si; 1=dsi/deta2; >1=dsi/deta2(eta2)]
-30.d0    eta2min     [eta of second hardest jet]
30.d0     eta2max

```

```

'=====
'      VEGAS and OUTPUT'
'=====
'----- VEGAS parameters -----
3000      ipoin      [No.  of points per integr.]
5         itt        [No.  of iterations]
10        iprn       [Printflag: 10=screen output]
1.d-5     eps        [Precision of int.]
'----- Name of output file -----
'test.out'jfileout   [Filename]

```

## Appendix B: Output-file

If the user chooses to calculate the spectrum of a variable, the output-file will contain the result in the following form:

5.0	1026.109741210937	4.70078134536743
6.0	513.3152465820313	2.41036343574524
7.0	284.2205505371094	1.30083477497101
8.0	164.3175811767578	.7139108777046204
9.0	101.2273483276367	.4778541326522827
10.0	64.58644104003906	.2957088351249695
11.0	42.4879379272461	.1964362561702728
12.0	29.31233406066895	.1275904476642609
13.0	20.39706230163574	9.869953989982605E-02
14.0	14.49518013000488	6.361690163612366E-02
15.0	10.62311935424805	4.653203114867210E-02

The first entry is the point in the spectrum (in this case the value of  $E_T$ ), the second entry is the resulting cross section in [pb] (here  $d\sigma/dE_T$ ) and the third entry gives the statistical errors of the VEGAS-integration in [pb].

If the user chooses to calculate a certain bin (by setting all integration variables, i.e., `iQ2`, `ipt`, `ieta1` and `ieta2`, equal to zero), the output-file will contain only one line, with the first number being zero:

.0	1691.092895507812	9.78220748901367
----	-------------------	------------------

The second entry again gives the cross section in the chosen bin in [pb] and the third entry gives the error. Note that the cross section is not normalized by the bin width.